

## In, Sn, Pb and Zn Contents and Their Relationships in Ore-forming Fluids from Some In-rich and In-poor Deposits in China

ZHANG Qian<sup>1,\*</sup>, ZHU Xiaoqing<sup>1</sup>, HE Yuliang<sup>1,2</sup> and ZHU Zhaohui<sup>1,2</sup>

<sup>1</sup> State Key Laboratory of Ore Deposit Geochemistry, Institute of Geochemistry, Chinese Academy of Sciences, Guiyang, Guizhou 550002

<sup>2</sup> Graduate School of the Chinese Academy of Sciences, Beijing 100039

**Abstract:** All the indium-rich deposits with indium contents in ores more than  $100 \times 10^{-6}$  seems to be of cassiterite-sulfide deposits or Sn-bearing Pb-Zn deposits, e.g., in the Dachang Sn deposit in Guangxi, the Dulong Sn-Zn deposit in Yunnan, and the Meng'entaolegai Ag-Pb-Zn deposit in Inner Mongolia, the indium contents in ores range from  $98 \times 10^{-6}$  to  $236 \times 10^{-6}$  and show a good positive correlation with contents of zinc and tin, and their correlation coefficients are 0.8781 and 0.7430, respectively. The indium contents from such Sn-poor deposits as the Fozichong Pb-Zn deposit in Guangxi and the Huanren Pb-Zn deposit in Liaoning are generally lower than  $10 \times 10^{-6}$ , i.e., whether tin is present or not in a deposit implies the enrichment extent of indium in ores. Whether the In enrichment itself in the ore-forming fluids or the ore-forming conditions has actually caused the enrichment/depletion of indium in the deposits? After studying the fluid inclusions in quartz crystallized at the main stage of mineralization of several In-rich and In-poor deposits in China, this paper analyzed the contents and studied the variation trend of In, Sn, Pb and Zn in the ore-forming fluids. The results show that the contents of lead and zinc in the ore-forming fluids of In-rich and -poor deposits are at the same level, and the lead contents range from  $22 \times 10^{-6}$  to  $81 \times 10^{-6}$  and zinc from  $164 \times 10^{-6}$  to  $309 \times 10^{-6}$ , while the contents of indium and tin in the ore-forming fluids of In-rich deposits are far higher than those of In-poor deposits, with a difference of 1–2 orders of magnitude. Indium and tin contents in ore-forming fluid of In-rich deposits are  $1.9 \times 10^{-6}$ – $4.1 \times 10^{-6}$  and  $7 \times 10^{-6}$ – $55 \times 10^{-6}$ , and there is a very good positive correlation between the two elements, with a correlation coefficient of 0.9552. Indium and tin contents in ore-forming fluid of In-poor deposits are  $0.03 \times 10^{-6}$ – $0.09 \times 10^{-6}$  and  $0.4 \times 10^{-6}$ – $2.0 \times 10^{-6}$ , respectively, and there is no apparent correlation between them. This indicates, on one hand, that In-rich ore-forming fluids are the material basis for the formation of In-rich deposits, and, on the other hand, tin probably played a very important role in the transport and enrichment of indium.

**Key words:** In-rich deposit, In-poor deposit, ore-forming fluid, fluid inclusion, ore-forming elements

### 1 Introduction

As viewed from the data available all over the world, In-rich ore deposits (The ores generally contain  $>100 \times 10^{-6}$  In.) are dominated by cassiterite-sulfide and Sn-bearing Pb-Zn deposits, and indium is present largely in sphalerite (Anderson, 1953; Ivanov et al., 1963; Greta, 1980; Murao et al., 1991; Zhang et al., 1998; Tsushima et al., 1999; Benzaazoua et al., 2003). This feature is referred to as specialities of In-enrichment mineralization type and In-enrichment mineral (Zhang et al., 2003). In-rich deposits have generally higher ore-forming temperatures, and are,

more or less, associated with intermediate-acidic magmatic activities, for example, cassiterite-sulfide deposits in the Dachang orefield of Guangxi, the Dulong orefield and Gejiu orefield of Yunnan, the Meng'entaolegai orefield of Inner Mongolia in China. Those Sn-barren Pb-Zn deposits that have high temperature and are related genetically to magmatism have very low contents of indium (The ore generally contains less than  $10 \times 10^{-6}$  In.) such as the Fozichong orefield of Guangxi, the Huanren orefield of Liaoning, the Shuikoushan orefield and Huangshaping orefield of Hunan. A typical example is that in the Dachang orefield, e.g., ores from the Sn-poor Lamo Cu-Zn deposit

\* Corresponding author. E-mail: zhqiangeol@163.com and zhuqxcas@sohu.com.

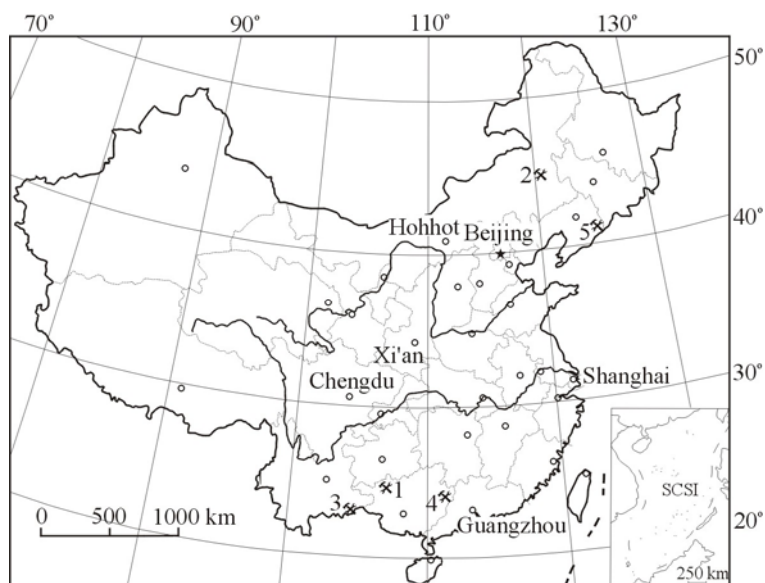


Fig. 1. Sketch map showing the distribution of some In-rich and In-poor deposits in China (Based on the 1/400 Geological Map of China by SinoMaps Press in 1989).

1. Dachang orefield in Guangxi; 2. Dulong Sn-Zn deposit in Yunnan; 3. Meng'entaolegai Ag-Pb-Zn deposit in Inner Mongolia; 4. Fozichong Pb-Zn orefield in Guangxi; 5. Huanren Pb-

contain only  $10 \times 10^{-6}$ – $15 \times 10^{-6}$  In, while those from the Sn-rich Changpo-Tongkeng, Longtoushan, Dafulou and Baotan deposits have high contents of more than  $100 \times 10^{-6}$  In, of which Orebody 100 in the Longtoushan deposit contains  $310 \times 10^{-6}$  In averagely. Zhang et al. (2003) deduced that (a) tin may play an important role in indium enrichment; (b) in the presence of tin, indium would be easily concentrated together in ore-forming fluids and transported together with tin, but in the process of precipitation and mineralization the two would be separated from each other, and tin often form tin minerals and indium entered mainly sphalerite. In order to attest these points of view, we analyzed the contents of indium and tin (including Pb and Zn) in ore-forming fluids of some In-rich and In-poor ore deposits in China and studied the relationship between these elements.

## 2 Geology of In-rich and In-poor Ore Deposits and Sample Selection

Ore deposits involved in this study mainly include Sn-rich sulfide deposits and Sn-poor Pb-Zn deposits. The former is enriched in indium, and the ores generally contain indium as much as  $100 \times 10^{-6}$  or more; the latter is depleted in indium, and the indium contents in ores are usually less than  $10 \times 10^{-6}$  (Zhang et al., 1998). Orebodies-91 and -92 in the Changpo-Tongkeng deposit of the Dachang orefield in Guangxi, the Meng'entaolegai Sn-bearing Ag-Pb-Zn deposit in Inner Mongolia, and the Dulong Sn-Zn deposit in

Yunnan are selected as typical In-rich deposits, while the Fozichong Pb-Zn deposit in Guangxi and the Huanren Pb-Zn deposit in Liaoning are selected as typical In-poor deposits. The distribution of these deposits is shown in Fig. 1.

### 2.1 Orebodies-91 and -92 in the Changpo-Tongkeng deposit

The Dachang Sn orefield is located at the joint of the NW tectonic zone and E-W tectonic zone on the southern margin of the Jiangnan Block, which consists of the Changpo-Tongkeng, Bali, Longtoushan, Dafulou, Maopingchong, Makeng, Lajiapo and Lamo deposits. With the exception of Lamo, all the other deposits are enriched in indium and the reserves reach more than 6000 t. The Changpo-Tongkeng deposit is the largest in scale with tin reserves accounting approximately for more than 50% of the total in the Dachang Sn orefield. The main ore-bearing rock series are the Middle-Upper Devonian series (Fig. 2a), and the orebodies are controlled by the NW-extending Dachang anticline. In the mining district, S-N-extending granite-porphyry dykes are developed.

Orebody-91 occurs in siliceous limestone of bed b in the second member of the Upper Devonian Series, extending about 500 m in the striking direction and about 1000 m in the dipping direction, with a thickness of 15 m on average. Orebody-92 occurs in siliceous rocks in the first member of the Upper Devonian Series, and its size is twice as large as that of orebody-91, with the maximum thickness reaching 86 m (Fig. 2a). Sn, Zn and Pb ores are dominant, associated with large amounts of useful elements such as Sb, In, Cd, Ag. By our analysis, the indium content in ore from the two orebodies is between  $50 \times 10^{-6}$ – $160 \times 10^{-6}$ ; and the In element exists mainly in sphalerite, with the In contents reaching  $350 \times 10^{-6}$  to  $2200 \times 10^{-6}$ .

Orebodies are composed predominantly of mineralized lamellar bands and veinlets (network veins), and the former is usually penetrated by the latter. In addition, there was developed a small amount of nodular and interlayered veined mineralization. Lamellar banded mineralization is composed of alternative lamellar bands differing in composition, constituting a typical lamellar structure. The lamellar bands are generally 0.1 mm to 10 mm thick, parallel to one another, and folded along with the strata. Sulfide-quartz lamellae, sulfide-tourmaline lamellae, carbonaceous muddy lamellae and siliceous lamellae can be distinguished, of which siliceous lamellae occupy the biggest proportion. The forms of mineralization within the orebodies are dominated by veinlet replacement (e.g.



Fig. 2. Geological sketch map of In-rich deposits

(a) Orebodies-91 and -92 in the Dachang orefield (Based on Huang and Tang, 1988): 1. clay ironstone of bed a in the third member of the Upper Devonian Series; 2. large lenticular limestone of bed d in the second member of the Upper Devonian Series; 3. small lenticular limestone of bed c in the second member of the Upper Devonian Series; 4. narrow banded limestone of bed b in the second member of the Upper Devonian Series; 5. wide banded limestone of bed a in the second member of the Upper Devonian Series; 6. chert in the first member of the Upper Devonian Series; 7. geological boundary; 8. fault; 9. orebody No.; 10. stratoid veinlet disseminated-metasomatic-type orebodies; 11. veinlet orebody.

(b) Dulong Sn-Zn deposit (Based on Liu et al., 1999): 1. mica-quartz schist intercalated with marble of the fifth member in the Middle Cambrian Tianpeng Formation; 2. marble intercalated with schist of the fourth member in the Tianpeng Formation; 3. mica-quartz schist intercalated with marble and skarn lenses of the third member in the Tianpeng Formation; 4. marble intercalated with schist and stratiform skarn of the second member in the Tianpeng Formation; 5. granulite and gneiss of the first member in the Tianpeng Formation; 6. two-mica granite; 7. granoporphyry; 8. fault; 9. geological boundary; 10. orebody.

(c) Meng'entaolegai Ag-Pb-Zn deposit (Based on Zhu et al., 2004): 1. biotite granite; 2. muscovite granite; 3. post-stage lamprophyre dyke; 4. geological boundary of lithological character; 5. fault; 6. orebody.

Orebody-91) and network dissemination replacement (e.g., Orebody-92). As the mineralization is bond within siliceous limestones and siliceous rocks, the orebodies are generally distributed in the stratoid form. Veinlets and network veins are closely spaced, with the most spaced location containing 18 veins per meter. The veins are generally 0.3–5 cm wide.

The metallic minerals are mainly cassiterite, pyrrhotite, marmatite, pyrite, arsenopyrite, jamesonite; the subordinate minerals are galena, siderite, stibnite, chalcocopyrite, stannite, marcasite, boulangerite, freibergite, matildite, scheelite,

native bismuth, etc. The non-metallic minerals include quartz, calcite, tourmaline, K-feldspar, muscovite, chlorite, etc. Ore textures are represented by euhedral, subhedral and euhedral-granular crystals. In addition, there are ring texture, filling texture, solid solution texture, porphyroblastic texture, grating texture, sub-graphic texture, relict texture, crushed texture, etc. Ore structures include veined, banded, miarolitic, boudinage, networked, massive, disseminated, mottled, lump, lamellar and brecciated structures.

Han and Shen (1994), Li and Lei (1994), Jiang et al.

(1999), Ye et al. (1999) and Fan et al. (2004) described geological and geochemical characteristics of the Dachang orefield and considered that this deposit was formed by sea-floor hydrothermal exhalative sedimentary-metallogenesis in the early stage and superimposed by Yanshanian magmatism in the late stage.

## 2.2 Dulong Sn-Zn deposit

This deposit is located in the western part of the Nanling fold zone and at the joint of the Yangtze block and the Ailaoshan fold zone. The exposed strata in the mining district are the Middle Cambrian Tianpeng Formation, its rocks on top part are mainly muddy dolomitic limestone and schist; and going downwards, the metamorphic degree is enhanced, which is characterized by the occurrence of granulite, biotite-plagioclase gneiss and granogneiss (Fig. 2b). The major orebodies occur in the schist-interbedded marble and layered skarn of the second member of the Tianpeng Formation. Regional magmatic activities were strong, and there is exposed the Laojunshan granite, 150 km<sup>2</sup>, in the northeastern part of the mining district, which yielded Rb-Sr isotopic ages ranging from 90 Ma to 118 Ma. Intruding along the SN-extending fault is a small granoporphry massif, whose muscovite K-Ar age is 76 Ma (Liu et al., 1999). The main ore-controlling fault system in the mining district is a set of S-N-extending faults and the main orebodies are distributed along the F<sub>1</sub> fault.

The ore-hosting skarn bodies are stratoid, lenticular and tubular in shape and mostly distributed in the marble on both sides of the fault system. The skarn minerals are dominated by actinolite, diopside, hedenbergite, tremolite, garnet, epidote, chlorite, etc. Skarnization is accompanied with varying-degree Sn-Zn mineralization and skarnization along both sides of the F<sub>1</sub> fault usually leading to the formation of industrial orebodies, which are consistent with the skarn rocks with respect to their shape (Fig. 2b). The proven tin reserves have reached 33×10<sup>4</sup> t, and Zn, 302×10<sup>4</sup> t, associated with a variety of elements such as Cu, Pb, Cd and In. The indium reserves is more than 5000 t, with the indium contents of 62×10<sup>-6</sup>–145×10<sup>-6</sup> in ores and 280×10<sup>-6</sup>–1430×10<sup>-6</sup> in sphalerite.

The main metallic minerals are marmatite, pyrrhotite, cassiterite, pyrite; and coming next are galena, magnetite, chalcopryrite, arsenopyrite, stibnite, stannine, etc. Non-metallic minerals include quartz, calcite and minor fluorite, plagioclase, etc. in addition to the skarn minerals mentioned above. The ore textures are mainly metablastic texture, relict texture, subhedral texture and anhedral-granular texture, metasomatic-resorption texture, metasomatic-relict texture, etc.; the ore structures include massive, disseminated, lamellar-banded, mottled, veined-networked and brecciated structures. In addition to

skarnization, silicification and carbonatization occurred at the hydrothermal stage.

Liu et al. (2000a, b) described the geological and geochemical characteristics of the Dulong deposit and they considered that the formation of this deposit experienced three stages, i.e., sea-floor hot-water sedimentation, regional metamorphism and magmatic hydrothermal superimposition. As the sphalerite Rb-Sr age of 76 Ma for this deposit (Liu et al., 1999) is consistent with that of the granite-porphry (79 Ma), and skarnization is closely related to mineralization, we suggest that magmatism played a more important role than sea-floor hot-water sedimentation and metamorphism in the formation of this deposit. The formation of the Furong Sn deposit in Hunan is also related to the acidic magmatism (Mao et al., 2004).

## 2.3 Meng'entaolegai Ag-Pb-Zn deposit

The Meng'entaolegai Ag-Pb-Zn deposit is located at the juncture of the Da Hinggan Uplift Zone and the Songliao Subsidence Zone in the east of Inner Mongolia. The deposit occurs in a set of E-W-extending faults at the center of a Hercynian granite batholith (Fig. 2c). The granite batholith is composed mainly of biotite-plagioclase granite and muscovite-plagioclase granite. The biotite-plagioclase granite is the main portion of the Meng'entaolegai granite massif, yielding a biotite K-Ar age of 281 Ma and a Rb-Sr isochron age of 246 Ma (Sheng et al., 1999). The muscovite-plagioclase granite intruded the biotite-plagioclase granite, with the muscovite K-Ar ages of 212–251 Ma (Sheng et al., 1999).

There are more than 40 orebodies in the whole mining district distributed in the western, middle and eastern ore runs. The individual orebodies are measured at 400–2000 m in length. The orebodies are veined in shape and their attitudes are consistent with those of fault structures (Fig. 2c). In the western segment of the mining district the V<sub>8</sub> orebody is dominant. The main metallic minerals are sphalerite, pyrite and minor amounts of galena and chalcopryrite. In the middle segment the V<sub>1</sub> orebody is dominated by Zn-Pb mineralization, which is enriched in Ag and the main metallic minerals are sphalerite and galena. Orebodies in the western and middle segments are enriched in indium and tin, with indium present largely in sphalerite and tin mainly in stannite. In the eastern segment the V<sub>11</sub> orebody is dominant, which is characterized by Pb-Ag mineralization. The reserves of Zn in the deposit amount of about 30×10<sup>4</sup> t or more, 15×10<sup>4</sup> t Pb, >2000 t Sn; 500 t In and 1800 t Ag. Indium contents in sphalerite are 300×10<sup>-6</sup> to 2600×10<sup>-6</sup>.

The main metallic minerals are galena, sphalerite, and large amounts of silver minerals, such as native silver, electrum, acanthite, pyrrargyrite, proustite, dyscrasite,

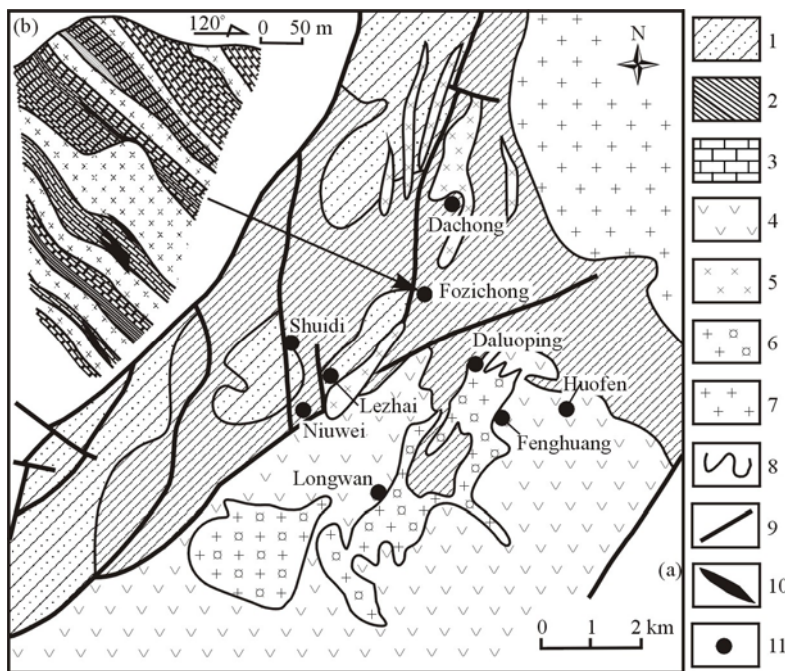


Fig. 3. Geological map of the Fozichong Pb-Zn orefield (Based on Zhang, 1992). (a) Distribution of the ore deposits in the Fozichong orefield; (b) Section map of the No.35 line of the Fozichong deposit; 1–3. Silurian strata: 1. sandstone; 2. shale (slate); 3. limestone; 4. dacite liparite; 5. Yanshanian granodiorite; 6. Late Yanshanian granoporphyry; 7. Hercynian granite; 8. fault; 9. geological boundary; 10. orebody; 11. ore deposit.

pyrostitpnite, stephanite, diaphorite, freibergite, etc. The non-metallic minerals are dominated by quartz and subordinated by calcite, siderite, sericite and chlorite.

Ore textures are mainly euhedral-subhedral-anhedral-granular textures, metasomatic resorption texture, metasomatic-relict texture and graphic texture; ore structures are dominated by massive and disseminated structures, banded structure, veined and networked structures, brecciated structure, and crushed structure. Wall-rock alterations are mainly silicification, sericitization, chloritization, carbonatization and Mn-carbonatization. The alterations were developed mainly along the fault structure, generally within the bounds of 1–15 m on both sides of a fault.

According to Zhu et al. (2004, 2006), the Meng'entaolegai deposit is a magmatic hydrothermal deposit genetically connected with Early Yanshanian magmatic activities.

#### 2.4 Fozichong Pb-Zn deposit

The Fozichong orefield is located within the Yunkai Caledonian Uplift Zone on the southern margin of the E-W-extending folded zone in the Nanling region. The strata are mainly Silurian sandstone and shale intercalated with limestone. In the northeast of the orefield, there is a Hercynian granite, whose whole-rock Rb-Sr age is 326 Ma; a Jurassic andesitic rhyolite is developed in the south, with a Rb-Sr age of 129 Ma. The granoporphyry that

intruded the rhyolite was dated at 75 Ma. The granodiorite distributed along the Niuwei fault was dated at 150 Ma (Zhang, 1993; Lei, 1995).

Two types of orebodies are developed in the orefield (Xu, 1995), i.e., the Fozichong-type skarn orebodies (including the Fozichong, Liutang, Longwan, Fenghuangchong, Huofen, etc.) and the Niuwei-type filling-replacement orebodies (including the Niuwei, Leizhai, Wulonggang, Shuidi, etc.), and the Fozichong-type orebodies are the dominant ones in the orefield. The orebodies are stratiform, stratoid and tubular in shape.

Wall-rock alterations are intense, including skarnization, diopsidization, hornblenization, silicification, chloritization, epidotization, etc. The ore deposits are closely related to the granoporphyry and granodiorite in space, and are mostly distributed near the contact zone of these magmatic rocks (Fig. 3). Individual orebodies generally extend as long as 200–

500 m, with the maximum up to 700 m, and they extend downwards 200–400 m and 1–4 m thick with the maximum value of 17 m.

The Niuwei-type orebodies occur in the foot-wall of the Niuwei fault and by the sides of the second-order fault. The country rocks are the Silurian sandstone and shale. The orebodies are veined, lenticular, chambered and irregular in shape, which generally measured at 10–15 m in thickness, 50–100 m in length and extend downwards 50–300 m. Wall-rock alterations are weak, e.g., diopsidization, chloritization, epidotization, silicification and marblization.

The two types of ore deposits are generally consistent in composition, predominated by Pb and Zn, associated with Ag and Cu. The deposits contain no Sn and are depleted in indium, and its contents are lower than  $10 \times 10^{-6}$  in ores and  $40 \times 10^{-6}$  in sphalerite. Metallic minerals in the ores are galena, sphalerite, marmatite, pyrite, pyrrotite, chalcopyrite, arsenopyrite, magnetite, marcasite, etc. Non-metallic minerals are diopside, tremolite, quartz, calcite, chlorite, actinolite, garnet, etc. In addition to veined and brecciated structures, banded, disseminated and massive structures are commonly seen; ore textures are dominated by euhedral and anhedral textures, metasomatic-relict texture, solid solution separated texture, crushed texture, etc.

The two types of orebodies are genetically connected with Yanshanian magmatic activities (Zhang, 1993; Lei et

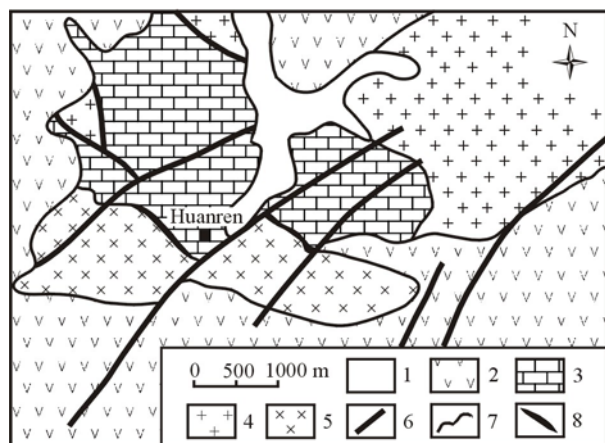


Fig. 4. Geological map of Huanren Pb-Zn deposit in Liaoning (Based on Zhang, 1993).

1. Quaternary; 2. Jurassic andesite; 3. Cambrian limestone; 4. Lüliangian migmatitic granite; 5. Yanshanian pyroxene diorite; 6. fault; 7. geological boundary; 8. orebody.

al., 2002).

## 2.5 Huanren Pb-Zn deposit

The Huanren Pb-Zn deposit is a skarn deposit closely associated with pyroxene diorite (Zhang, 1992). It is located at the terminal of the Yan-liao Subsidence Zone in the hanging wall of the subduction zone on the western bank of the Pacific Plate. The strata exposed in the mining district are mainly Jurassic andesite and Cambrian carbonate rocks. Magmatic activities include those represented by Precambrian (Lüliangian) migmatitic granites, Jurassic andesitic volcanic activities and those marked by the intrusion of pyroxene diorite in addition to the intrusion of some granoporphyritic veins. At the contact of the pyroxene diorite with the Cambrian limestone, strong skarnization is observed, resulting in large-scale skarn massifs (Fig. 4). From the skarn massifs to the country rocks there can be distinguished skarnized diorite, epidote skarn, epidote-garnet skarn, diopside-garnet skarn and skarnized marble. The form of the skarn massifs is in consistency with the attitude of the contact zone. The orebodies are mostly veined, lenticular, chambered and stratoid in shape, generally several hundred meters long, 2–6 m wide and 100–300 m deep, which occur mainly within the skarn massifs, and their forms are controlled by the skarn massifs.

The useful elements contained in the Huanren deposit are Pb, Zn, Ag, Cu and Fe (magnetite), showing an obvious zonation. The Pb-Zn-Ag orebody is located in the upper part or in the exocontact zone, the Cu-Zn orebody is located in the middle part or in the contact zone, and the Fe-Cu orebody is located in the deep part or in the endocontact zone. The ores contain no tin and less than  $10 \times 10^{-6}$  indium. The main metallic minerals include

magnetite, chalcocopyrite, galena, sphalerite and pyrite. Coming next are pyrrhotite, bornite, chalcocite, hematite, tetrahedrite, native silver, acanthite, etc. The main gangue minerals are garnet, diopside, actinolite, calcite, quartz, epidote, chlorite, sericite, etc. Ore textures are dominated by granular texture, metasomatic-resorption texture, metasomatic-relict texture; ore structures are dominated by massive, disseminated, banded, veined, networked, mottled, and brecciated structures. Wall-rock alterations include silicification, chloritization, carbonatization and sericitization at the hydrothermal stage. All the alterations are closely related to mineralization.

## 3 Analytical Method and Results

### 3.1 Sample

The seventeen ore samples were collected from the main orebodies of the selected deposits, and their characteristics and In, Sn, Pb, Zn contents measured by ICP-MS are listed in Table 1. As indium is present mainly in sphalerite, coexisting quartz is selected for the analysis of the ore-forming elements in fluid inclusions in order to prevent pollution of indium and the other ore-forming elements in the sphalerite from being leached out in the process of sample pre-treatment.

Samples were all examined under microscope prior to ore dressing so as to determine their mineral compositions, textures, structures, and mineral cogenetic relations and confirm that the quartz and metallic sulfides are of cogenesis. On this basis, the samples were prepared as polished fluid inclusion slices to study the types of fluid inclusions so as to determine their size, quantity and type, distinguish primary fluid inclusions and measure the homogenization temperatures. The results showed that quartz fluid inclusions in these deposits are large in amount and big in size (generally within the range of 5–30  $\mu\text{m}$ ). V-L two phase fluid inclusions are dominant and their homogenization temperatures are relatively high, generally higher than 250  $^{\circ}\text{C}$ , with the maximum value even up to 400–450  $^{\circ}\text{C}$  (Table 2). A minor amount of secondary fluid inclusions can be seen locally in quartz from the Dachang, Dulong, Meng'entaolegai and Fozichong deposits (generally less than 10  $\mu\text{m}$  in size, mostly between 1–5  $\mu\text{m}$ , linearly arrayed, homogenization temperatures lower than 200  $^{\circ}\text{C}$ ).

### 3.2 Sample treatment

Su et al. (2001) successfully measured the contents of REE and ore-forming elements in fluids from quartz fluid inclusions in Carlin-type gold deposits of Guizhou Province, and established a complete set of sample treatment and analytical procedures. So in this study

**Table 1 Characteristics and major element contents of ore samples from indium-rich and -poor ore deposits**

Deposit type	Deposit	Sample No.	Occurrence	Sample characteristics	In	Sn	Zn	Pb	Zn/Pb
In-rich deposits	Changpo-Tongkeng deposit in Dachang, Guangxi	GD-10	Orebody 92	Sph-Py-Cas-Qtz massive ore	132	0.46	14.84	1.66	8.94
		GD-14	Orebody 91	Py-Sph-Cas-Qtz ore	185	0.74	16.23	0.82	19.79
		GD-21	Orebody 91	Py-Sph-Cas-Qtz ore	194	0.67	15.99	1.2	13.33
		GD-31	Orebody 91	Py-Sph-Cas-Qtz ore	236	0.63	21.05	2.11	9.98
	Meng'entaolegai, Inner Mongolia	M-8	Orebody V8	Sph-Gal-Qtz massive ore	123	0.31	9.54	4.43	2.15
		M-20	Orebody V8	Sph-Gal-Py-Qtz massive ore	179	0.42	17.68	3.29	5.37
		M-21	Orebody V1	Sph-Gal-Qtz ore	123	0.39	15.22	3.18	4.79
		M-25	Orebody V1	Sid-Sph-Gal-Qtz ore	149	0.18	11.01	5.79	1.90
		M-34	Orebody V11	Sph-Gal-Py-Qtz ore	98	0.13	12.6	3.89	3.24
	Dulong Sn-Zn deposit, Yunnan	MJ-56	Open mining yard at Manjiazai	Qtz-Sph-Cas-Cp ore	138	0.48	14.63	1.68	8.71
		MJ-58	Open mining yard at Manjiazai	Qtz-Sph-Cas massive ore	147	0.29	15.16	0.37	40.97
In-poor deposits	Fozichong Pb-Zn deposit, Guangxi	F-9	Niuwei	Qtz-Sph-Gal disseminated ore	11	0.006	17.31	3.94	4.39
		F-23	Daozhikou	Qtz-Sph-Gal disseminated ore	8	0.002	13.56	3.25	4.17
		F-26	Daozhikou	Qtz-Sph-Gal disseminated ore	12	0.005	21.04	4.22	4.99
		F-33	Daozhikou	Qtz-Sph-Gal disseminated ore	4	0.001	23.97	3.01	7.96
	Huanren Pb-Zn deposit, Liaoning	LW-12	Main orebody	Gal-Sph-Qtz ore	5	0.001	8.55	7.09	1.21
		LW-24	Main orebody	Gal-Sph-Qtz ore	3	0.003	6.94	5.96	1.16

Sph-sphalerite; Gal-galena; Py-pyrite; Cas-cassiterite; Qtz-quartz; Cp-chalcopyrite; Sid-siderite. Analytical method: In, by ICP-MS; Sn, by polarography; Pb and Zn, by routine chemical methods. Unit: In ( $\times 10^{-6}$ ); Sn, Pb and Zn (%).

**Table 2 Characteristics and homogenization temperatures of quartz fluid inclusions in both In-rich and In-poor deposits**

Deposit	Sample No.	Characteristics and types of fluid inclusions	Shape	Size ( $\mu\text{m}$ )	V/L ratio (%)	$T_{\text{H}}$ ( $^{\circ}\text{C}$ )
Changpo-Tongkeng	GD-10, GD-14, GD-21	Randomly occurring within quartz, in large amounts	Elliptic, rounded irregular	3–15	10–20	250–405
Meng'entaolegai	M-8, M-20, M-25, etc.	In the center of quartz grains, distributed in groups	Rounded-elliptic, elongated, irregular	5–20	10–30	255–420
Dulong	MJ-56, MJ-58	L+V, Distributed randomly, in large amounts	Elliptic, irregular	5–15	15–20	263–390
Fozichong	F-9, F-23, F-33	L+V, Distributed in groups or scatters, in large amounts	Elongated elliptic, rounded and irregular	10–20	10–20	248–451
Huanren	LW-12, LW-24	L+V, Occurring randomly, scattered locally	Rounded, elliptic and irregular	10–25	15–30	280–440

Fluid inclusion types in these deposits include pure liquid phase inclusions in addition to vapor/liquid double-phase inclusions. Daughter mineral fluid inclusions are occasionally seen. The Huanren deposit also contains methane inclusions. As fluid inclusions in most of the deposits have been specially investigated, this study is focused only on the size, type, quantity and homogenization temperature and genesis of fluid inclusions in the collected samples.

similar methods were employed.

The ore samples were first crushed and quartz grains were handpicked. Selected quartz was crushed as fine as 80–40 mesh (0.2–0.4 mm) and washed to remove most sulfides. Then, 6 g of pure quartz was picked out under the microscope, of which 3 g was used for analysis and the other 3 g for standby. The quartz minerals reached the purity of 99%.

3 g of the selected quartz was boiled with highly pure  $\text{HNO}_3$  for 5–10 hours at the temperature of  $200\text{ }^{\circ}\text{C}$  so as to dissolve the impurities on the surface or in the fissures of quartz to remove part of the secondary fluid inclusions in it. Then, twice deionized water was used to wash the quartz samples times till the electric conductivity of the washing liquid reached that of twice deionized water. After that, the quartz sample was baked for 12 hours till dryness at low temperature to completely eliminate the moisture on the surface of quartz grain.

### 3.3 Extracted fluid

Su et al. (2001) made comparisons of advantages and disadvantages for the different ways of opening fluid inclusions, and considered that the decrepitated method was the best choice. As the ore-forming temperatures for the selected deposits are generally within the range of  $250\text{--}400\text{ }^{\circ}\text{C}$  and a few secondary fluid inclusions were formed below  $200\text{ }^{\circ}\text{C}$ , two steps were involved in the opening of fluid inclusions. Firstly, quartz sample was put into a high-temperature U-shaped quartz tube and decrepitated for 3–5 min at  $250\text{ }^{\circ}\text{C}$ . The quartz sample was then taken out, washed with 5%  $\text{HNO}_3$  till it was clean enough and baked till dryness at low temperature. The aim of this step is to remove low-temperature secondary fluid inclusions as thoroughly as possible. Secondly, the baked quartz sample was put into a new Ne-filled high-temperature U-shaped quartz tube and decrepitated for 5 min at  $650\text{ }^{\circ}\text{C}$ . Then the quartz fluid inclusions were opened for precision gas chromatographic analysis of the

**Table 3 ICP-MS operating parameters**

Function	Parameter	Function	Parameter	Function	Parameter
Ignition capability	1.2 kW	Sample input speed rate	1.0 mL/min	Scanning mode	Peak jump
Reflection capability	<2 W	Fore vacuum	2.31 cPa	Mass range	7–250
Ar gas speed rate of atomizer	0.64 L/min	High vacuum	10–90 $\mu$ Pa	Scanning time	20
Supplementary Ar gas speed rate	0.60 L/min	Retaining time at the sampling site	0.001 s	Number of sampling localities for each peak	10
Cooling gas speed rate	14.0 L/min	Resolution power	300	Integrated time for each mass	50 ms

**Table 4 Contents of the major metallic elements in quartz fluid inclusions ( $\times 10^{-6}$ )**

Deposit type	Deposit	Sample No.	Mineral	In	Sn	Zn	Pb	Zn/Pb
In-rich deposit	Changpo-Tongkeng deposit	GD-10	Quartz	3.6	37	208	35	5.94
		GD-14	Quartz	3.3	39	221	33	6.70
		GD-21	Quartz	2.7	19	216	48	4.50
		GD-31	Quartz	4.1	55	309	52	5.94
	Meng'entaolegai deposit	M-8	Quartz	2.8	21	195	62	3.15
		M-20	Quartz	3.5	36	294	58	5.07
		M-21	Quartz	2.4	14	268	66	4.06
		M-25	Quartz	2.9	15	194	73	2.66
		M-34	Quartz	1.9	7	211	54	3.91
	Dulong deposit	MJ-56	Quartz	2.5	17	211	43	4.91
MJ-58		Quartz	3.1	28	234	22	10.64	
In-poor deposit	Fozichong Pb-Zn deposit	F-9	Quartz	0.03	2	217	49	4.43
		F-23	Quartz	0.03	0.9	188	31	6.06
		F-26	Quartz	0.05	1.1	229	58	3.95
		F-33	Quartz	0.08	1.4	257	47	5.47
	Huanren Pb-Zn deposit	LW-12	Quartz	0.09	0.4	164	74	2.22
		LW-24	Quartz	0.06	0.6	179	81	2.21

Characteristics of samples see the Table 1.

contents of H<sub>2</sub>O in fluid inclusions. 5 mL of highly pure 5% HNO<sub>3</sub> leaching solution was added in the decrepitated sample, followed by the extraction of fluids from fluid inclusions via ultrasonic vibration and centrifugal separation for analysis.

### 3.4 Analytical conditions and results

Employed analytical instrument in this study was an ELEMENT-type high-resolution Inductively Coupled Plasma Mass Spectrometer (ICP-MS) made by the Finnigan MAT Company. The instrumental conditions are consistent with the parameters used in determining the contents of trace elements in quartz fluid inclusions from the Carlin-type gold ores in Guizhou by Su et al. (2001) (Table 3). The concentration value limit corresponding to the tri-folded standard deviation obtained by ten times of continuous determination of the blank solution in the whole experimental procedure is taken as the determination limit of the instrument. The determination limits of In, Sn, Pb and Zn are taken as 0.02 ng/g, 0.08 ng/g,

0.2 ng/g and 0.45 ng/g, respectively; and the blank value of the leaching solution refers to the contents of the elements mentioned above in the 5% HNO<sub>3</sub> solution used to soak fluid inclusions. The average values for 5 times of analysis are In 0.04 ng/g, Sn 0.11 ng/g, Pb 0.03 ng/g and Zn 0.51 ng/g, respectively. It can be seen that the blank values of the leaching solution and the instrumental determination limits are lower than  $1 \times 10^{-9}$ , which are far lower than their contents in fluid inclusion.

Under the above conditions, ICP-MS is used to analyze the contents of In, Sn, Pb and Zn in the prepared samples. The analytical results were converted to their contents in H<sub>2</sub>O in fluid inclusion determined by gas chromatographic analysis. The results of continuous 3 times of analysis for every sample are of well consistent and far higher than the blank values of the leaching solution and the instrumental determination limits. This indicates that the experiment is successful and the analytical result is credible. The average element contents are listed in Table 4. For the convenience of comparison with their contents in ores

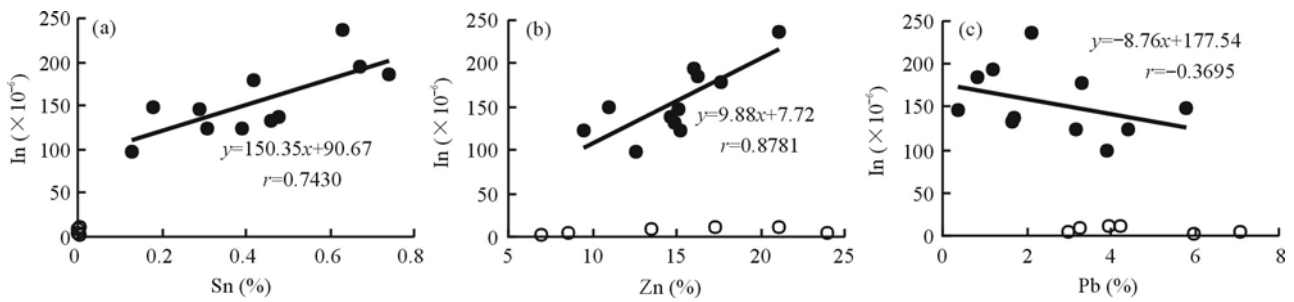


Fig. 5. Plots showing the relationship between In and Sn (a), Zn (b) and Pb (c) in the ores. Solid circles indicate In-rich deposits; open circles stand for In-poor deposits.

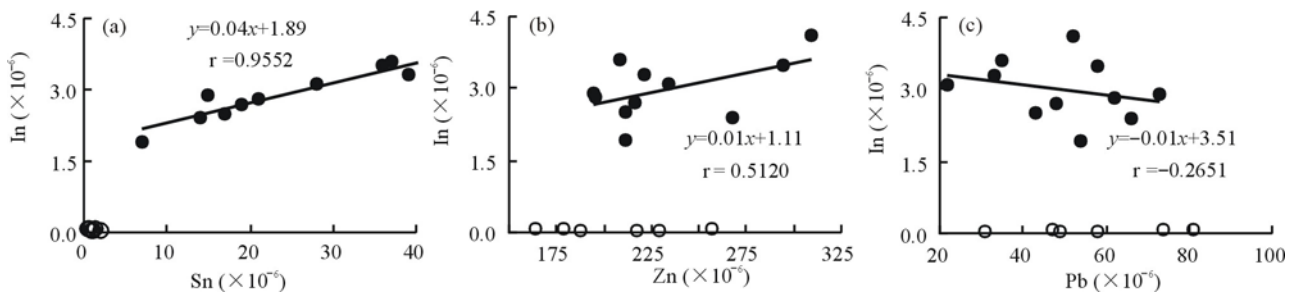


Fig. 6. Plots showing the relationships between In and Sn(a), Zn(b) and Pb (c) in ore-forming fluids. Solid circles indicate In-rich deposits; open circles stand for In-poor deposits.

listed in Table 1, the units of elements in Table 4 are expressed in  $\times 10^{-6}$ .

## 4 Results and Discussion

### 4.1 Contents of In, Sn, Pb and Zn and their relationships in ores

Table 1 shows that although the two types of ore deposits are different in the contents of Sn and In, both Pb and Zn are their major components. It is not hard to see that ores from the In-rich deposits contain indium of  $132 \times 10^{-6}$ – $236 \times 10^{-6}$  for the Changpo-Tongkeng deposit,  $98 \times 10^{-6}$ – $179 \times 10^{-6}$  for the Meng'entaolegai deposit and  $138 \times 10^{-6}$ – $147 \times 10^{-6}$  for the Dulong deposit, while those from the In-poor deposits contain less than  $10 \times 10^{-6}$  In. Another outstanding feature is that ores from the In-rich deposits are obviously enriched in tin, while the contents of tin in ores from the In-poor deposit are two orders of magnitude lower than those of the former.

As can be seen from Fig. 5, indium contents of ores from In-rich deposits show positive correlations with Sn and Zn, and the correlative coefficients are 0.7430 and 0.8781, respectively (Fig. 5a, 5b), but there is no such synchronous variation trend between In and Pb (Fig. 5c), which indicates that In is related mainly to Sn and Zn.

### 4.2 Contents of In, Sn, Pb and Zn and their relationships in ore-forming fluids

According to Table 4, lead and zinc are enriched in ore-

forming fluids from either In-rich or In-poor deposits and have no large variation between two types of deposits, with  $22 \times 10^{-6}$ – $81 \times 10^{-6}$  Pb and  $164 \times 10^{-6}$ – $309 \times 10^{-6}$  Zn. This is in good consistency with the fact that ores of the two types of deposits are enriched in lead and zinc.

Ore-forming fluids from the In-rich and In-poor deposits are distinctively different in the contents of indium and tin. The contents of tin in the ore-forming fluids from In-rich deposits are within the range of  $7 \times 10^{-6}$ – $55 \times 10^{-6}$ , while those in In-poor deposits, only  $0.4 \times 10^{-6}$ – $2 \times 10^{-6}$ , and the latter's tin contents are higher than the former's by 1–2 orders of magnitude. This difference is in accord with that in tin contents for the two types of ore deposits as listed in Table 1.

Table 4 shows that ore-forming fluids from In-rich deposits contain indium as much as  $1.9 \times 10^{-6}$ – $4.1 \times 10^{-6}$ . This content range is higher than the Clarke value ( $0.01 \times 10^{-6}$ ) by two orders of magnitude. While ore-forming fluids from In-poor deposits contain almost no indium ( $0.0 \times 10^{-6}$ ), the contents of indium are close to the Clarke value of the earth's crust and lower than those of indium in ore-forming fluids from In-rich deposits by two orders of magnitude. That is to say, ore-forming fluids from In-rich deposits are highly enriched in indium by a factor of  $>100$  times as compared with those from In-poor deposits.

In the ore-forming fluids indium and tin show very good linear variations, and the correlation coefficient reaches 0.9552 for In-rich deposits (Fig. 6a). There is a better

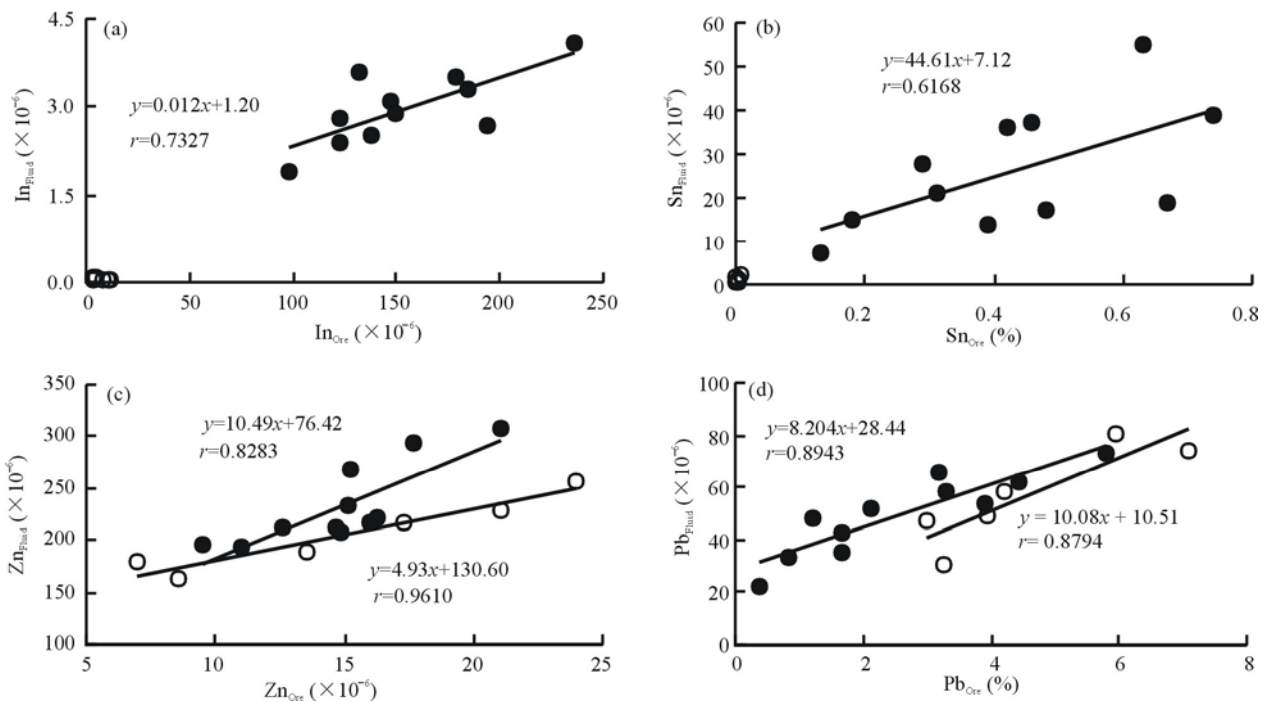


Fig. 7. The correspondence relationships between In (a), Sn (b), Zn (c) and Pb (d) in ore-forming fluids and ores. Solid circles indicate In-rich deposits; open circles stand for In-poor deposits.

correlation between indium and zinc, with the correlation coefficient of 0.5120 (Fig. 6b), but no correlation between indium and lead (Fig. 6c). The correlation coefficient between indium and tin in ore-forming fluid is larger than that in ores, while two coefficients between indium and zinc in ore-forming fluid and in ores show itself the contrary tendency with indium and tin, indicating that indium has the affinity with tin in fluid and it is related to zinc in ores.

The ore-forming fluids for In-poor deposits are depleted in both indium and tin, with no obvious correlation between the two elements (Fig. 6a).

The geological fact that when the contents of tin in the In-rich deposits and the related ore-forming fluids are high, the contents of indium are also high, seems to indicate that in the case of the existence of tin in large amounts, indium would be possible to enter the ore-forming fluids in large amounts to lay down the foundation for the enrichment and ore formation of indium. This is just in consistency with the deduction of Zhang et al. (2003) that the enrichment and ore formation of indium is closely related to tin.

#### 4.3 Corresponding relations of In, Sn, Pb and Zn between ore-forming fluids and ores

It is obvious that the elements not present in the ore-forming fluids can not appear in the ores, whereas those appear in the ore-forming fluids would not necessarily gathered as ores in the deposits. This problem can be deciphered by comparing the contents of ore-forming

elements in the fluids with those in the ores. From Fig. 7, the contents of ore-forming elements in the ores always depend on these in the ore-forming fluids. Either in In-rich deposits or in In-poor deposits, both Pb and Zn are the useful metallic elements in the ores; in case the contents of lead and zinc are high in the ore-forming fluids, they will be high in the ores, both showing a very good synchronously increasing trend. Either on the whole, or individually, these two types of ore deposits display the same variation trend (Fig. 7c, d).

From Fig. 7a and 7b, the simultaneous enrichment of indium and tin and their simultaneous depletion in the ore-forming fluids and ores from In-rich and In-poor deposits can distinctively separate these two types of deposits from each other. This indicates probably that the enrichment of indium and tin in the ores depends remarkably on whether the two metallic elements are present or not in the ore-forming fluids and their quantities. What is different is that indium in the ore-forming fluids for In-rich deposits shows a linear positive correlation with indium in the ores, with the correlation coefficient of 0.7327 (Fig. 7a), while the correlation of tin in the ore-forming fluids and in ores is poorer than that of indium in two phases, with the correlation coefficient of 0.6168 (Fig. 7b).

#### 4.4 Role of tin in the process of indium enrichment

A hard fact is that all In-rich deposits are Sn-rich deposits as well (Murao et al., 1991; Zhang et al., 1998). In China some In-rich deposits are all cassiterite-sulfide deposits,

e.g., the Dachang orefield of Guangxi, the Dulong orefield and Gejiu orefield of Yunnan, the Meng'entaolegai orefield of Inner Mongolia, the Xitieshan orefield of Qinghai and the Yinshan orefield of Jiangxi. (Huang et al., 1998; Zhang et al., 1998). According to the research of Greta (1980), in some coal mines of Bulgaria, the indium contents of coal are up to  $20 \times 10^{-6}$ – $167 \times 10^{-6}$ , with the maximum value of  $1000 \times 10^{-6}$ , and some cassiterite-sulfide deposits are also enriched in indium. Sphalerite and Cu-Fe-Sn-S-containing sulfide minerals in the Nakakoshi cassiterite-sulfide deposit of Japan contain 1.8%–16.3% indium, and the ores contain 0.02% In on average, which is thus a typical In-rich deposit (Tsushima et al., 1999). The presence of In-bearing sphalerite in the ore deposits in the Gasborn region of central Switzerland make the deposits enriched in indium (Kieft and Damman, 1990), etc. In these In-rich deposits the most common metallic elements associated with Sn are Cu, Zn, Pb and Sb. But there has been no report about the presence of indium in Sn-barren Cu, Zn, Pb and Sb deposits. The simultaneous enrichment and depletion of indium and tin in the ores and ore-forming fluids from both In-rich and In-poor deposits indicate that tin has played a very important role in the enrichment and migration of indium.

Seward et al. (2000) described the properties of the complexes of indium chloride in hydrothermal solutions at 25–350 °C and under saturated vapor pressure conditions, as well as the variation characteristics of In-Cl and In-O bonds with respect to their length and pointed out that the hydrates of chlorides of indium [ $\text{In}(\text{ClO}_4)(\text{H}_2\text{O})_5^{2+}$  and  $\text{InCl}_n(\text{H}_2\text{O})^{3-n}_{6-n}$ ] played an important role in the migration of indium in the hydrothermal system. However, in fact, in the geological processes the environment of indium is more complicated than that of pure indium-chloride systems. If indium migrates merely in the form of simple In-chloride, it could be enriched in the deposits of any element assemblage. The contents of indium and other ore-forming elements in ore-forming fluids and their relationships indicate that the existence of In-rich ore-forming fluids is the materials basis for the formation of In-rich deposits. As deduced from the data available, In-rich ore-forming fluids appear to be able to form only in case that tin is present in large amounts in fluids.

In oxidation state, indium seems to be a siderophile element. Based on our analytical results, it is often enriched in Fe-bearing rock-forming minerals such as biotite, hornblende and sometimes in limonite. They have the similar geochemical character under oxidation condition and In-Sn alloy is manufactured in the material industry based on their similar chemical property. Indium is usually modified and transferred under oxidation state in the geological process. Therefore, we infer that when tin exists in a hydrothermal system, indium and tin jointly form a

certain complex compound and transferred together; and this compound is indispensable to the enrichment of indium. However, their idiographic migratory form, medium property and type of complex compound need further research. It is incontrovertible that the key of answering this question depends on the experiment of indium-tin-related elements coexisting system and determination of their complex compound types.

In the hydrothermal system, indium is a strongly chalcophile (sulphophile) element. It seldom forms indium minerals and usually replaces other elements in Zn-Cu-Sn-bearing minerals, which are similar in ionic radius to that of indium (Yi et al., 1995). Trivalent indium ( $\text{In}^{3+}$ ), when 6-coordinated, has an ionic radius of 0.081 nm, close to the ionic radius of  $\text{Zn}^{2+}$ . When indium is precipitated, it is usually enriched in sulfides of zinc. Tin is considered a siderophile element and is usually present in the form of cassiterite in the sulfide deposits. In most cases, cassiterite contains a lower amount of indium (Yang, 1990), but in some complex tin-bearing sulphide minerals, the contents of indium could be relatively high. This indicates that the foremost sulphophile property of indium is prominent in the reductive hydrothermal condition. Though indium has intimate relation with tin in fluids, it mainly enters sulfur-bearing minerals when it precipitates in the reductive condition. According to Liu et al. (1984), indium has very strong selectivity to its carrier minerals and then it preferentially enters a few of sulfide minerals that have hexahedron structure. Therefore, the well-known In-rich deposits over the world are those of Sn-Pb-Zn-Cu-Sb-Ag coexistence, and no matter what element assemblage exists, tin in the deposit is indispensable (Yi et al., 1995; Anderson, 1953; Ivanov et al., 1963; Radkevich et al., 1963; Pearce et al., 1984; Johan, 1988; Pattrick et al., 1993; Botelho and Moura, 1998; Benzaazoua et al., 2003; Zhang et al., 2003).

## 5 Conclusions

The most significant difference between In-rich and In-poor ore deposits is whether there exists tin or not. The In-rich ore deposits are dominated by cassiterite-sulfide deposits and Sn-bearing Pb-Zn deposits. Indium contents in ores of this type of deposits are more than  $100 \times 10^{-6}$ , and there is a positive correlation between indium and zinc, and also between indium and tin, with correlation coefficients of 0.8781 and 0.7430, respectively. In-poor ore deposits are characterized by a trace amount of tin, and ores contain indium less than  $10 \times 10^{-6}$ .

The two types of deposits also show differences in contents of indium and tin in their ore-forming fluids, i.e., the contents of indium and tin in the ore-forming fluids for In-rich deposits are obviously higher than those in the ore-

forming fluids for In-poor deposits, with a difference by 1–2 orders of magnitude; there is a very good correlation between indium and tin in the former, with a correlation coefficient of 0.9552. This indicates that (1) the existence of the In-rich ore-forming fluid can provide the material foundation for the formation of the In-rich deposits, and (2) simultaneous enrichment of indium and tin in the ore-forming fluid of the In-rich deposit, and simultaneous indigence of them in that of the In-poor deposit indicate that tin plays a very important role in the migration and enrichment of indium. It is deduced that the presence of tin is more favorable to the incorporation of indium into fluids to form In- and Sn-bearing ore-forming fluids. The two metallic elements are transported together; but in the process of precipitation indium is incorporated mainly into sphalerite or sulphide minerals of tin; and only in a few cases (e.g., in the case of pressure and temperature drop), a part of indium would be incorporated into cassiterite.

Seward et al. (2000) held that indium migrates mainly in the form of chlorides of indium, but In-rich deposits usually have very complex element associations (e.g., Cu, Pb, Zn, Ag and Sb), especially the close relationship between indium and tin. So, more experiments are necessary before the occurrence and the migration of indium in ore-forming fluids can be further verified.

## Acknowledgements

We wish to thank Prof. Pan Jiayong at the Open Laboratory of Endogenic Metallic Ore Deposits of Nanjing University, Associate Prof. Su Wenchao of the Institute of Geochemistry, Chinese Academy of Sciences for their efforts in ore-forming element analysis of mineral fluid inclusions and sample treatment, and Associated Profs. Qi Liang and Yang Qishun as well as Senior Engineer Feng Jiayi of the Institute of Geochemistry, Chinese Academy of Sciences for their hard work in the analysis and measurement of In, Sn, Pb, and Zn in ores and ore-forming fluids. Thanks are also given to the Key Orientation Research Project of the Chinese Academy of Sciences (KZCX2-YW-111), the National Natural Science Foundation of China (Grant Nos. 40172037 and 40072036) for its financial support.

Manuscript received Dec. 12, 2005

accepted July 3, 2006

edited by Xie Guanglian and Zhang Xinyuan

## References

- Anderson, J.S., 1953. Observations on the geochemistry of indium. *Geochim. Cosmochim. Acta*, 4: 225–240.
- Benzaazoua, M., Marion, L.P., Pinto, L.A., Migeon, H., and Wagner, F.E., 2003. Tin and indium mineralogy within selected samples from the Neves Corvo ore deposit (Portugal): a multidisciplinary study. *Minerals Engineering*, 16: 1291–1302.
- Botelho, N.F., and Moura, M.A., 1998. Granite-ore deposit relationships in central Brazil. *J. S. Am. Earth Sci.*, 11: 427–438.
- Fan, D., Zhang, T., Ye, J., Pasava, J., Kribek, B., Dobes, P., Varrin, I., and Zak, K., 2004. Geochemistry and origin of tin-polymetallic sulfide deposits hosted by the Devonian black shale series near Dachang, Guangxi, China. *Ore Geology Reviews*, 24: 103–120.
- Greta, M.E., 1980. On the geochemistry of indium in coal-forming processes. *Geochim. Cosmochim. Acta*, 44: 1023–1027.
- Han Fa and Shen Jianzhong, 1994. Silica and oxygen stable isotopic geochemistry of Dachang tin deposit. *Acta Mineralogica Sinica*, 14: 172–180 (in Chinese with English abstract).
- Huang Minzhi and Tang Shaohua, 1988. *Ore Petrology on Tin Field Deposits at Dachang*. Beijing: Beijing Science and Technology Publishing House, 176 (in Chinese with English Abstract).
- Huang Song, Zhou Weining and Zhang Jinzhang, 1998. The occurring state and comprehensive utilization assessment of Cd, Ga and In in the Yingshan Pb-Zn deposit, Jiangxi. *J. Guilin Inst. Tech.*, 18: 22–27 (in Chinese with English abstract).
- Ivanov, V.V., Rodionov, D.A., Tarkhov, and Yu.A., 1963. Character of the distribution and the average content of indium in some minerals from deposits of various genetic types. *Geochemistry*, 11: 1056–1067.
- Jiang, S.-Y., Han, F., Shen, J.-Z., and Palmer, M.R., 1999. Chemical and Rb-Sr, Sm-Nd isotopic system of tourmaline from the Dachang Sn-polymetallic ore deposit, Guangxi Province, P. R. China. *Chem. Geol.*, 157: 49–67.
- Johan, Z., 1988. Indium and germanium in the structure of sphalerite: An example of coupled substitution with copper. *Mineral. Petrol.*, 39: 211–229.
- Kieft, K., and Damman, A. H., 1990. Indium-bearing chalcopyrite and sphalerite from the Gasborn area, West Bergslagen, Central Sweden. *Mineral. Mag.*, 54: 109–112.
- Lei Liangqi, 1995. Dating and geochemistry of the magmatic rocks in the Fozichong Pb-Zn(Ag) Mining Field, Guangxi, China. *Acta Petrologica Sinica*, 11: 77–82 (in Chinese with English abstract).
- Lei Liangqi, Song Ci'an, and Feng Zhuohai, 2002. Discussion on Multi-element Enrichment Characteristics and Genesis of Fozichong Pb-Zn(Ag) Metallogenic Belt, Guangxi. *Mineral Deposits*, 21: 74–82 (in Chinese with English abstract).
- Li Youxi and Lei Yuanqing, 1994. Relationship between the Upper Devonian Famennian lithofacies and paleo-geography and the tin-multimetal ore in the Dachang area, Guangxi. *Journal of Stratigraphy*, 18: 53–56 (in Chinese with English abstract).
- Liu Yingjun, Cao Liming, Li Zhaolin, Wang Henian, Chu Tongqing and Zhang Jingrong, 1984. *Element Geochemistry*. Beijing: Science Press, 387–393 (in Chinese).
- Liu Yuping, Li Chaoyang, Zeng Zhigang and Wang Jinliang, 1999. Mono-mineral Rb-Sr Dating Contour Determination of Dulong tin and zinc deposit. *Journal of Kunming Technical*

- College of Metallurgy*, 15: 5–8 (in Chinese with English abstract).
- Liu Yuping, Li Chaoyang and Liu Jiajun, 2000a. Characteristics and genesis of stratiform skarn from Dulong tin-zinc polymetallic deposit, Yunnan. *Acta Mineralogica Sinica*, 20: 378–384 (in Chinese with English abstract).
- Liu Yuping, Li Chaoyang, Gu Tuan and Wang Jianliang, 2000b. Isotopic constraints on the source of ore-forming materials of Dulong Sn-Zn polymetallic deposit, Yunnan. *Geology-Geochemistry*, 29: 75–82 (in Chinese with English abstract).
- Mao Jingwen, Li Xiaofeng, Chen Wen, Lan Xiaoming and Wei Shaoliu, 2004. Geological characteristics of the Furong tin orefield, Hunan,  $^{40}\text{Ar}/^{39}\text{Ar}$  dating of tin ores and related granite and its geodynamic significance for rock and ore formation. *Acta Geologica Sinica* (English edition), 78: 481–491.
- Murao, S., Masaroni, F., and Uchida, A.C., 1991. Geology of indium deposits—a review. *Mining Geology*, 41: 1–13.
- Patrick, R.A.D., Dorling, M., and Poly, D.A., 1993. TEM study of indium- and copper-bearing growth-banded sphalerite. *Can. Mineral.*, 31: 105–117.
- Pearce, J.A., Harris, N.B.W., and Tindle, A.G., 1984. Trace element discrimination diagrams for the tectonic interpretation of granitic rocks. *J. Geol.*, 25: 956–983.
- Radkevich, R.O., Klintsova, A.P., and Kotle'nikova, L.L., 1963. Geochemistry of sphalerites of the Sadon deposit (Northern Caucasus). *Geokhimiya*, 5: 460–469.
- Seward, T.M., Henderson, C.M.B., and Charnock, J.M., 2000. Indium (III) chloride complexing and solvation in hydrothermal solutions to 350°C: an EXAFS study. *Chem. Geol.*, 167: 117–127.
- Sheng Jifu, Li Yan and Fan Shuyi, 1999. A study of minor elements in minerals from polymetallic deposits in the central part of the Dahingan mountains. *Mineral Deposits*, 18: 153–160 (in Chinese with English abstract).
- Su Wenchao, Hu Ruizhong, Qi Liang and Fang Weixuan, 2001. Trace elements in fluid inclusions in the Carlin-type gold deposits, south-western Guizhou Province. *Chinese J. Geochem.*, 20: 233–239.
- Tsushima, N., Matsueda, H., and Ishihara, S., 1999. Poly-metallic mineralization at the Nakakoshi copper deposits, Central Hokkaido, Japan. *Resource Geology*, 49: 89–97.
- Xu Hai, 1995. The study of mineralization model and exploration model in Fozichong area, Guangxi. *Geological Exploration for Non-Ferrous Metals*, 4: 341–345 (in Chinese with English abstract).
- Yang Shiyu, 1990. The spatio-temporal distributions and ore-forming model of the tin deposits in south-east Yunnan. *Scientia Geologica Sinica*, (2): 138–140 (in Chinese with English abstract).
- Ye Xusun, Yan Yunxiu and He Haizhou, 1999. The mineralization factors and tectonic evolution of Dachang superlarge tin deposit, Guangxi, China. *Geochimica*, 28: 213–221 (in Chinese with English abstract).
- Yi, W., Halliday, A.N., Lee, D.-C., and Christensen, J.N., 1995. Indium and tin in basalts, sulfides, and the mantle. *Geochim. Cosmochim. Acta*, 59: 5081–5090.
- Zhang Qian, 1992. Geochemistry of the Huanren skarn-type Cu-Pb-Zn poly-metallic deposit in Liaoning Province, China. *Geochimica*, 21: 243–254 (in Chinese with English abstract).
- Zhang Qian, 1993. Characteristics of isotopes and trace elements and genesis of the Hesun Pb-Zn orefield, Guangxi, China. *Geological exploration for Non-Ferrous Metals*, 2: 247–253 (in Chinese with English abstract).
- Zhang Qian, Zhan Xinzhi, Pan Jiayong and Shao Shuxun, 1998. Geochemical enrichment and mineralization of indium. *Chinese J. Geochem.*, 17: 221–225.
- Zhang Qian, Liu Zhihao, Zhan Xinzhi and Shao Shuxun, 2003. Specialization of ore deposit types and minerals for enrichment of indium. *Mineral Deposits*, 22: 309–316 (in Chinese with English abstract).
- Zhu Xiaoqing, Zhang Qian, He Yuliang and Zhan Xinzhi, 2004. A Study on the genesis of the Meng'entaolegai Indium-rich Multi-metallic Deposit in Inner Mongolia. *Mineral Deposits*, 23: 52–60 (in Chinese with English abstract).
- Zhu, X., Zhang, Q., He, Y., Zhu, C., and Huang, Y., 2006. Hydrothermal source rocks of the Meng'entaolegai Ag-Pb-Zn deposit in the granite batholith, Inner Mongolia, China: constrained by isotopic geochemistry. *Geochem. J.*, 40: 265–275.